BMC Cancer

RESEARCH Open Access

GLO1 regulates hepatocellular carcinoma proliferation and migration through the cell cycle pathway

Yao Zhang[1,2,3†], Xiaolong Tang[1,2,3†], Lin Liu[1,2,3†], Dan Cai[1,2,3], Shuang Gou[1,2,3], Siyu Hao[1,2,3], Yan Li[5], Jing Shen[1,2,3], Yu Chen[1,2,3], Yueshui Zhao[1,2,3], Xu Wu[1,2,3], Mingxing Li[1,2,3], Meijuan Chen[1], Xiaobing Li[1], Yuhong Sun[1], Li Gu[1], Wanping Li[1], Fang Wang[1], Zhuo Zhang[6], Xiaodong Wang[7], Shuai Deng[1,2,3], Zhangang Xiao[1,2,3,4*], Lei Yao[8,9*] and Fukuan Du[1,2,3*]

Abstract

Background Hepatocellular carcinoma (HCC) is a malignant tumor characterized by a high mortality rate. The occurrence and progression of HCC are linked to oxidative stress. Glyoxalase-1 (GLO1) plays an important role in regulating oxidative stress, yet the underlying mechanism remains unclear. GLO1 may serve as a prognostic biomarker and therapeutic target for HCC.

Methods Based on TCGA database hepatocellular carcinoma samples, we conducted a bioinformatics analysis to explore the correlation between GLO1 expression and HCC cell proliferation and viability. Kyoto Encyclopedia of Genes and Genomes (KEGG) pathway enrichment analysis revealed that differentially expressed genes (DEGs) were mainly enriched in the cell cycle pathway. We analyzed the relationships between GLO1 and 24 genes enriched in the cell cycle pathway using a protein-protein interaction (PPI) network. Finally, experimental validation was performed to assess GLO1's impact on the distribution of cells at different cell cycle stages and on the proliferation and migration of HCC cells.

Results Our study demonstrated that GLO1 was overexpressed in HCC tissues and was associated with a poor prognosis. Data analysis indicated that overexpression of GLO1 activated the cell cycle pathway and positively correlated with expression of the majority of key cell cycle genes. Experimental validation showed that GLO1 expression affects the number of HCC cells in G2 and S phases and regulates HCC cell proliferation and migration.

†Yao Zhang, Xiaolong Tang and Lin Liu contributed equally to this work and share first authorship.

*Correspondence:
Zhangang Xiao
zhangangxiao@swmu.edu.cn
Lei Yao
yaolei2009@gmail.com
Fukuan Du
adublg@126.com

Full list of author information is available at the end of the article

Conclusions GLO1 represents a promising therapeutic target for HCC, providing valuable insights into its role in the viability and proliferation of HCC cells.

Keywords *GLO1*, Hepatocellular carcinoma, Cell cycle, Biomarker, Therapeutic target

Introduction

GLO1 is a cytoplasmic glutathione-dependent enzyme that detoxifies the glycolysis by-product methylglyoxal. Methylglyoxal is a cancer metabolite involved in metabolic reprogramming [1]. *GLO1* plays a crucial role in tumorigenesis and the progression of various cancers. The mechanism of *GLO1*-mediated regulation of targeted cancer cells has garnered substantial attention [2–12]. While *GLO1* is closely associated with cancer occurrence and development, its potential value as a therapeutic target for liver cancer treatment remains unexplored [13, 14]. Currently, comprehensive research on the role of GLO1 in HCC development is lacking, and existing findings require further validation.

According to global cancer statistics for 2020, liver cancer is the sixth-most common cancer in the world, with the third highest mortality rate and the fifth highest incidence [15]. Numerous factors contribute to liver cancer development, including hepatitis infections (HBV, HCV), alcohol consumption, obesity, diabetes mellitus, aflatoxin ingestion, non-alcoholic fatty liver disease, and metabolic syndrome [16–19]. Oxidative stress is a significant factor in carcinogenesis, playing a pivotal role in the development and progression of liver cancer of various etiologies [20–25]. Previous studies suggest that GLO1 is involved in the regulation of oxidative stress [26–29]. Given its role in oxidative stress regulation, *GLO1* may be a potential target for cancer therapy [30].

This study aims to investigate the role of *GLO1* in HCC and explore its potential as a prognostic biomarker and therapeutic target. We found that GLO1 expression levels were elevated in HCC tissues compared to normal tissues, with significant differences in survival associated with GLO1 expression. Kyoto Encyclopedia of Genes and Genomes (KEGG) pathway enrichment analysis and Gene Ontology (GO) enrichment analysis were utilized to elucidate the biological processes and pathways associated with *GLO1*. Our results indicate that *GLO1* contributes to the development of HCC by influencing the cell cycle pathway. Experimental verification further revealed that *GLO1* predominantly affects the G2 and S phase of the HCC cell cycle and regulates HCC cell proliferation and migration. This study proposes a new therapeutic target for the treatment of HCC and clarifies the molecular mechanism of HCC development.

Methods

Data sources

GLO1 expression levels and clinical HCC data were obtained from The Cancer Genome Atlas (TCGA) (http://cancergenome.nih.gov) [31]. Standardized TCGA and GTEX transcriptome data from normal tissue ($N=160$) and tumor tissue ($N=374$) samples were sourced from the UCSC database (https://xenabrowser.net/). The datasets GSE45436 ($N=39$, T = 95), GSE57957 ($N=39$, T = 39), and GSE76427 ($N=52$, T = 115), containing liver cancer sequencing data, were downloaded from the Gene Expression Omnibus (GEO) database (http://www.ncbi.nlm.nih.gov/geo/).

Analysis of *GLO1* mutations in HCC

The cBioPortal online site is an open-source platform with multidimensional cancer genomic datasets and clinical data sources for exploration, visualization, and analysis [32]. We utilized the cBioPortal tool to analyze *GLO1* mutations in HCC.

Survival analysis and HCC clinicopathological features

The "survival" and "survminer" R software packages were employed for survival analysis, and the Kaplan-Meier plotter assessed the association between GLO1 expression and patient survival in HCC [33]. Additionally, the clinicopathological data corresponding to the HCC samples were downloaded from TCGA and analyzed using R. The Kruskal-Wallis rank sum test identified significant differences ($p<0.05$).

Relationship between *GLO1* expression and immune cell infiltration

The ESTIMATE method inferred the ratio of stromal cells to immune cells in tumor samples, and the "estimate" R software package evaluated the stromal score, immune score, estimated score, and tumor purity [34]. The Tumor Immunity Estimation Resource (TIMER, https://cistrome.shinyapps.io/timer/) enables systematic integrated correlation analysis of tumor-infiltrating immune cell features and selected pivotal genes [35]. We evaluated GLO1 expression levels in HCC tissues and analyzed their relationship with tumor purity and six types of infiltrating immune cells. Additionally, to explore the potential relationship between *GLO1* expression and immune cell infiltration in HCC, we estimated the content of 22 immune cells using the CIBERSORT tool. Values of $p<0.05$ were considered statistically significant.

Table 1 Primer sequences for GLOI-sgRNA

gene	Primer sequences
GLO1-sgRNA-F	5′-CACCGACTCTACTTCTTGGCTTATC-3′
GLO1-sgRNA-R	5′-AAACCATAAGCCAAGAAGTAGAGTC-3′

Differentially expressed genes and pathway analysis

The HCC transcriptome data were analyzed using the limma package. The filter conditions to identify differentially expressed genes (DEGs) were as follows: fold change > |0.5|; adjusted $p<0.05$. The Database for Annotation, Visualization and Integrated Discovery (DAVID; http://david.abcc.ncifcrf.gov/) was used to perform GO and KEGG pathway enrichment analyses of DEGs.

Protein-protein interaction (PPI) network analysis

A protein-protein interaction (PPI) network graphically represents the physical and functional interactions between proteins in cells, constructed based on experimental data and computational predictions. NetworkAnalyst (https://www.networkanalyst.ca) is a tissue type–specific or cell type–specific protein-protein interaction (PPI) network analysis platform. The network integration algorithm uses the following bioinformatics tools: PPI networks, gene co-expression networks, and gene regulation networks [36]. We utilized NetworkAnalyst to construct a PPI network based on the relationships between *GLO1* and proteins associated with the cell cycle.

Cell culture

Human Hep3B and Huh-7 cells were provided by the School of Biomedical Sciences at the Chinese University of Hong Kong. The cells were cultured in DMEM (Thermo Fisher Scientific, USA) supplemented with 10% fetal bovine serum (FBS; Thermo Fisher Scientific) and penicillin/streptomycin (1:100; Gibco, Thermo Fisher Scientific). All cells were grown at 37 °C in an incubator with 5% CO2 (SHEL LAB, USA).

Plasmid construction

GLO1-specific gRNA was designed using the Best CRISPR Design Tool for Knockouts (https://www.synthego.com/products/bioinformatics/crispr-design-tool) (TSINGKE, Chengdu, China). The process involved linearizing the plasmid backbone, annealing the gRNA, ligating the annealed oligonucleotides into the linearized vector, transforming the ligation product into Stbl3 cells, and verifying the gRNA sequence. The gRNA sequence is shown in Table 1. The overexpression plasmid was designed by Beijing Haichuangkeye Biological Technology Co., Ltd. (Beijing, China).

Table 2 The primer sequences

Primer name	Forward Sequence (5′-3′)	Reverse Sequence (5′-3′)
GLO1	CACTCTACTTCTTTGGCTTATGAGG	GGGTCTCATCA TCTTCAGTGCC
18sRNA	AAGTCCCTGCCCTTTGTACACA	GATCCGAGGG CCTCACTAAAC

Construction of *GLO1* knockout and overexpression cell models

The lentivirus packaging system, along with the helper plasmids PspAX2 and PMD2.G, was used to transfect the target plasmid into HEK293T cells. The virus-containing cell supernatant was collected 48 h and 72 h after transfection, mixed, and centrifuged to concentrate the virus particles using PEG8000. The knockout group and the negative control for the knockout group were denoted "sgGLO1" and "sgNC", respectively; the overexpression group and its control were denoted "*GLO1*" and "control", respectively. To obtain a stable cell line, HCC cells were screened using puromycin (2 μg/mL) 2 d after transfection.

Quantitative real-time polymerase chain reaction

Total RNA was extracted from HCC cells using TRIzol reagent (Thermo Fisher Scientific, Waltham, MA, USA). Reverse transcription was conducted using the FastKing RT Kit (TIANGEN, Chengdu, China) to produce cDNA. Quantitative real-time polymerase chain reaction (qRT-PCR; reaction volume: 10 μL) was performed using the 2× TSINGKE Master qPCR Mix (SYBR Green I) kit (TSINGKE, Beijing, China). *18s* RNA was used as an internal reference. All primers were obtained from TSINGKE (Beijing, China; Table 2). mRNA expression levels were determined using the $2^{-\Delta\Delta Ct}$ method.

Western blot analysis

Total protein was extracted from HCC cells using 1 mM PMSF RIPA lysis buffer (Solarbio, China) and quantified using the BCA Protein Assay Kit (Beyotime, China). The protein lysate (80 μg) was denatured at 90 °C for 5 min in sodium dodecyl sulfate-polyacrylamide gel electrophoresis (SDS-PAGE) protein loading buffer (Beyotime, China). Samples were separated by 10% SDS-PAGE and transferred onto polyvinylidene fluoride membranes (Millipore, USA; IBFP0813C). The membranes were blocked with 5% non-fat milk in PBST for 1 h at room temperature and incubated overnight at 4 °C with primary anti-*GLO1* antibody (1:1000 dilution, rabbit; Abcam, ab81461) and primary anti–β-actin antibody (1:2000 dilution, mouse; Beyotime, AF0003). The membranes were then washed three times with PBST and incubated with anti-rabbit IgG (1:2000 dilution; Beyotime; A0208)

and anti-mouse IgG (1:2000 dilution; Beyotime; A0216) for 1 h at room temperature.

Cell proliferation assay

Cell suspensions from the four groups were inoculated into a 96-well culture plate at a density of 2000 cells per well and cultured at 37 °C in a 5% CO2 incubator. After 24, 48, 72, and 96 h of incubation, 90 μL of medium and 10 μL of cell counting kit-8 (CCK8) reagent (Dojindo, China) were added to each well. The cells were then incubated for an additional 2 h in the dark. The optical density of each well was measured at 460 nm using a microplate reader (Bio-Rad, Hercules, CA, USA, TY2018000102). Three wells were analyzed per group.

Wound healing assay

Cells (20×10^4) were seeded onto a six-well plate and incubated for 24 h until they reached confluence. The monolayer was scratched with a 10 μL pipette tip and washed with PBS to remove isolated cells. The cells were cultured in serum-free medium, and 4–5 images of the migration distance were captured in the same position for each well under an inverted fluorescence microscope (Nikon, Japan, Ts2R-FL) after 0, 24, and 48 h. The migration distance was calculated using ImageJ software.

Transwell invasion assay

The invasion assay was performed using a Transwell chamber (JETBIOFIL, Guangzhou, China) coated with Matrigel (Corning, Guangzhou, China). Transfected Hep3B and Huh-7 cells were suspended in serum-free medium and inoculated at a density of 2×10^4 cells per well into the upper chamber. The lower chamber contained medium supplemented with 10% FBS. After 48 h of incubation, the cells were fixed and stained with crystal violet. Photographs were taken under an inverted light microscope, and the invaded cells were counted using ImageJ software.

Flow cytometry analysis

Flow cytometry was performed to analyze the distribution of cells at different stages in the cell cycle. Cells in the logarithmic growth phase were inoculated uniformly into a six-well plate at a density of 2×10^4 cells per well and incubated in serum-free medium for 12 h. Next, the cells were transferred to complete medium and incubated for 48 h, after which they were washed with ice-cold PBS. Trypsin-digested cells were collected in a 1.5 mL conical tube and centrifuged at 1000 rpm for 3 min to obtain a precipitate. The cells were washed twice with ice-cold PBS and fixed with 75% ice-cold ethanol at -20℃ for 24 h. The cells were centrifuged, resuspended in PBS, treated with 50 μg/mL propidium iodide (PI) and 50 μg/mL RNase, and incubated at 37 °C for 30 min. Flow cytometry results (BD FACSVerseTM, USA) were analyzed using ModFit software.

In vivo experiments

Early zebrafish embryos (AB strain) were reared in Danien's buffer containing 10 mmol/L phenylthiourea at 28.5 ℃ on a 10 h/14 h light/dark cycle. All HCC cell lines and culture conditions were established as previously described. HCC cells were stained with DiI (Biyuntian Biotech Co., Ltd, C1036) red fluorescent dye for 1 h before injection and then resuspended in PBS at a concentration of 1×104 cells/μL. Embryos were anesthetized by administering 0.05 mg/mL tricaine (ethyl 3-aminobenzoate methanesulfonate, Sigma). HCC cells (5–20 nL per embryo) were injected into the yolk space using a pneumatic pico pump syringe with a glass microinjection needle. Tumor size was quantified by fluorescence microscopy, and the cells were incubated for 3 days.

Statistical analysis

All experiments were repeated three times for accuracy. GraphPad Prism 7.0.0 software was used for paired group data analysis. Student's t-test was used for statistical analysis. The threshold for statistical significance was set at $p<0.05$.

Results

GLO1 protein is highly expressed in HCC

We analyzed *GLO1* expression levels in HCC and normal tissues using mRNA expression data from TCGA and the GTEX database. We validated *GLO1* expression in three GEO datasets. *GLO1* mRNA expression was significantly higher in HCC samples than in normal tissues (Fig. 1A, C). Using the Human Protein Atlas Database, we compare *GLO1* protein expression in HCC and normal tissues (Fig. 1B), confirming high GLO1 protein levels in HCC tissues.

GLO1 alterations in HCC

Based on DNA sequencing data, we identified the type and frequency of *GLO1* mutations among HCC patients using the cBioPortal tool. The frequency of GLO1 alterations in HCC patients was 4%, including missense mutations (green), amplifications (red), and truncating mutations (light blue). Amplifications were the most frequent mutation type (Supplementary Fig. 2A). Supplementary Fig. 2B illustrates *GLO1* mutation sites in HCC. Additionally, we investigated whether overall survival (OS) and disease-free survival (DFS) were associated with GLO1 mutations. HCC patients were divided into an altered group ($n=13$) and an unaltered group ($n=353$) based on cBioPortal data. Kaplan-Meier curves plotted OS and DFS (Supplementary Fig. 2C). *GLO1* mutations

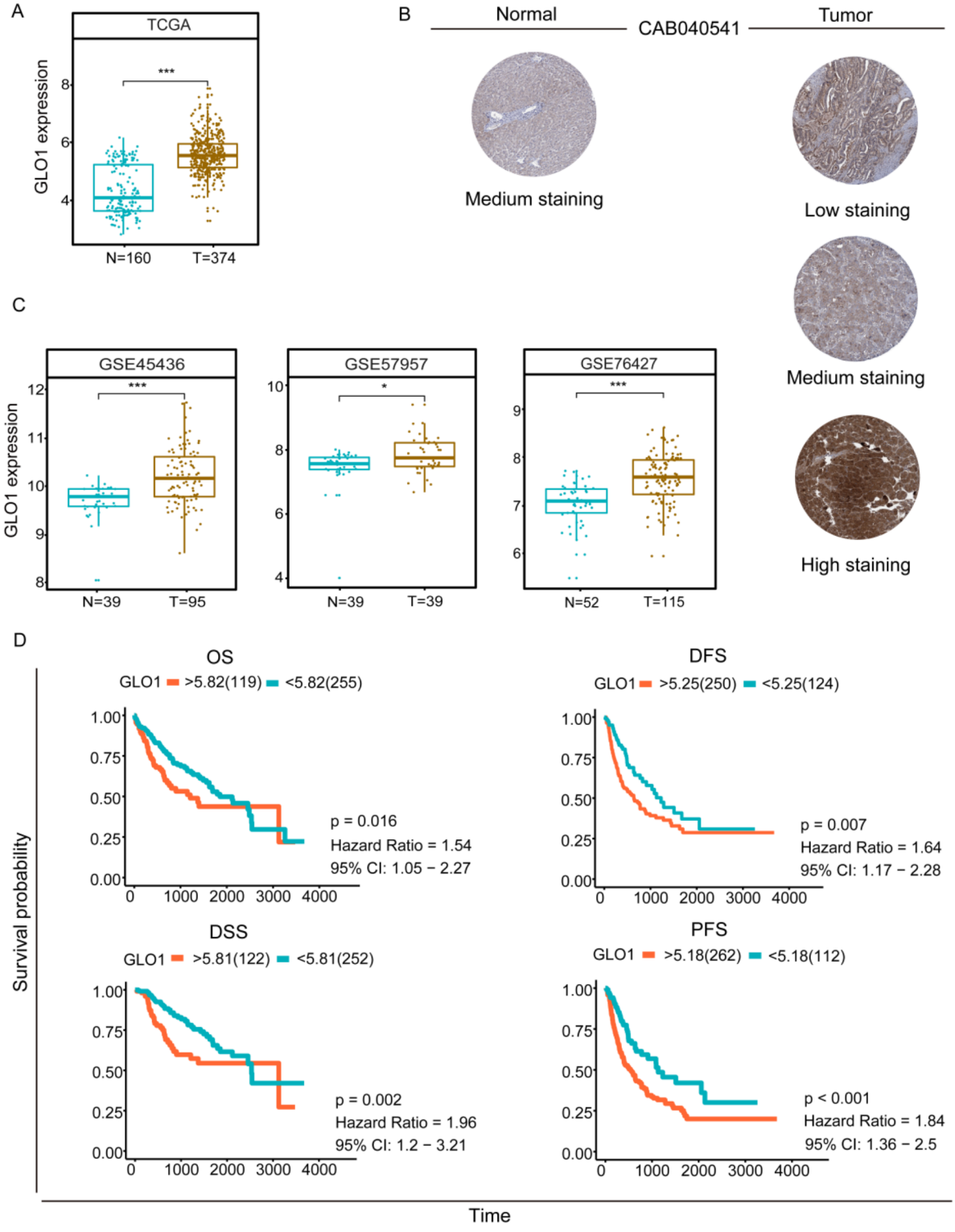

Fig. 1 *GLO1* expression levels and survival analysis in HCC. (**A**) Comparison of *GLO1* expression levels in HCC tissues and normal tissues was investigated by TCGA database. *$p < 0.5$, **$p < 0.01$, ***$p < 0.001$ between the two groups. (**B**) Protein levels from the Human Protein Atlas (HPA) assay *GLO1* in normal and HCC tumor tissues. (**C**) *GLO1* expression levels in HCC tissues compared to normal tissues verified by the GEO database. Between the two groups *$p < 0.5$, **$p < 0.01$, ***$p < 0.001$. (**D**) Kaplan-Meier survival analysis based on high and low *GLO1* expression. overall survival (OS), disease-free survival (DFS), disease-specific survival (DSS), and progression-free survival (PFS)

were not significantly associated with OS ($p=0.266$) or DFS ($p=0.722$).

High *GLO1* expression predicts poor prognosis in HCC patients

We aimed to verify if *GLO1* expression could serve as a prognostic biomarker in HCC patients. We conducted OS, DFS, disease-specific survival (DSS), and progression-free survival (PFS) analyses of *GLO1* in HCC using TCGA database. Kaplan-Meier analysis indicated that high *GLO1* expression was significantly associated with poor prognosis (Fig. 1D). The relationship between *GLO1* expression level and HCC stage, patient age, and patient sex was assessed using the Kruskal-Wallis rank sum test with Bonferroni adjustment. A significant association was found between *GLO1* expression and stages 1 and 3 (adjusted $p<0.05$), but no significant associations with other clinical factors (Supplementary Fig. 1). In conclusion, high *GLO1* expression is a risk factor for poor prognosis in HCC patients.

GLO1 is negatively and secondarily associated with immune infiltration in HCC

Oxidative stress can influence the immune response [37–40]. Given *GLO1*'s close association with oxidative stress, we hypothesized that *GLO1* regulates the immune response and participates in immune surveillance. In addition, *GLO1* participates in immune surveillance and immune cell infiltration control in another human malignancy [12]. *GLO1* expression varied with HCC immune and stromal scores (Fig. 2A); it was negatively correlated with the immune score (r = -0.25, $p=1\times10^{-6}$) and stromal score (r = -0.4, $p<2.2\times10^{-6}$) (Fig. 2B). The correlation between *GLO1* expression and stromal score was stronger than with the immune score. We then explored the relationship between *GLO1* expression and immune cell infiltration levels. *GLO1* expression showed a weak positive correlation with tumor purity ($r=0.267$, $p=4.58\times10^{-7}$) and macrophage content ($r=0.239$, $p=8.43\times10^{-6}$). *GLO1* expression also exhibited a very weak positive correlation with the content of B cells ($r=0.158$, $p=3.36\times10^{-3}$), CD8+T cells ($r=0.107$, $p=4.87\times10^{-2}$), CD4+T cells ($r=0.118$, $p=2.84\times10^{-2}$), neutrophils ($r=0.191$, $p=3.63\times10^{-4}$) and dendritic cells ($r=0.166$, $p=2.12\times10^{-3}$) (Fig. 2C). These results indicate that *GLO1* plays a minor role in HCC immune cell infiltration.

GLO1 expression is associated with tumor cell viability and proliferation

Patients were categorized into high and low groups based on GLO1 expression scores. Expression profiles were compared, revealing 458 DEGs related to GLO1. To elucidate the functional role of *GLO1* in HCC, we performed functional enrichment analysis of 458 DEGs using the DAVID platform (Fig. 3A, B; Supplementary Table 1). GO enrichment analysis showed that, among molecular function (MF) terms, the DEGs were enriched in "protein binding" and "protein homodimerization activity"; among cellular component (CC) terms, they were enriched in "nucleus" and "extracellular exosome"; and among biological process (BP) terms, they were enriched in "cell division" and "mitotic nuclear division" (Fig. 3C and Supplementary Table2). KEGG pathway analysis revealed that the DEGs were mainly enriched in "cell cycle", "biosynthesis of antibiotics", and "DNA replication" (Fig. 3D and Supplementary Table 2).

GLO1 regulates cell cycle pathway

To explore the transcription relationship between *GLO1* and 24 genes enriched in the cell cycle pathway, we used the "ggpubr" package to perform correlation analysis at the transcriptional level in liver cancer. The expression of 23 genes was positively correlated with *GLO1* expression: *E2F1*, *CDC6*, *CDK1*, *SKP2*, *TTK*, *PCNA*, *CDC20*, *PTTG1*, *MCM2*, *CDC25C*, *MCM3*, *BUB1B*, *MCM4*, *SMC3*, *MCM5*, *MCM6*, *CCNB1*, *CDC45*, *MCM7*, *CCNB2*, *PLK1*, *BUBI*, and *CCNA2*. *GADD45B* expression was negatively correlated with *GLO1* expression (Fig. 4A). To further explore the potential interactions between these 24 genes and *GLO1*, a PPI network was constructed using the NetworkAnalyst tool (Fig. 4B).

GLO1 knockout and overexpression affect the HCC cell cycle

Bioinformatics analysis indicated a potential association between *GLO1* expression and the cell cycle. To study the effect of *GLO1* expression on the HCC cell cycle, we knocked out and overexpressed *GLO1* in Hep3B and Huh-7 cells via lentiviral transduction and verified the efficiency of knockout and overexpression by qRT-PCR and western blotting (Fig. 5A, B, and C). We analyzed the distribution of cells in different cell cycle stages via flow cytometry and PI staining. Knockout and overexpression of *GLO1* affected the number of Hep3B and Huh-7 cells in G2 and S phases. In *GLO1*-knockout cells, the number of cells in the G2 phase increased, the number of cells in the S phase decreased, and there was no significant change in the number of cells in the G1 phase. In *GLO1*-overexpressing cells, the number of cells in the G2 phase decreased, the number of cells in the S phase increased, and there was no significant change in the number of cells in the G1 phase (Fig. 6). These data indicated that *GLO1* affected the number of HCC cells in G2 and S phases. Given that *GLO1*'s influence on these phases is critical for DNA replication and subsequent mitosis, we aim to further investigate whether *GLO1* affects HCC cell proliferation and migration.

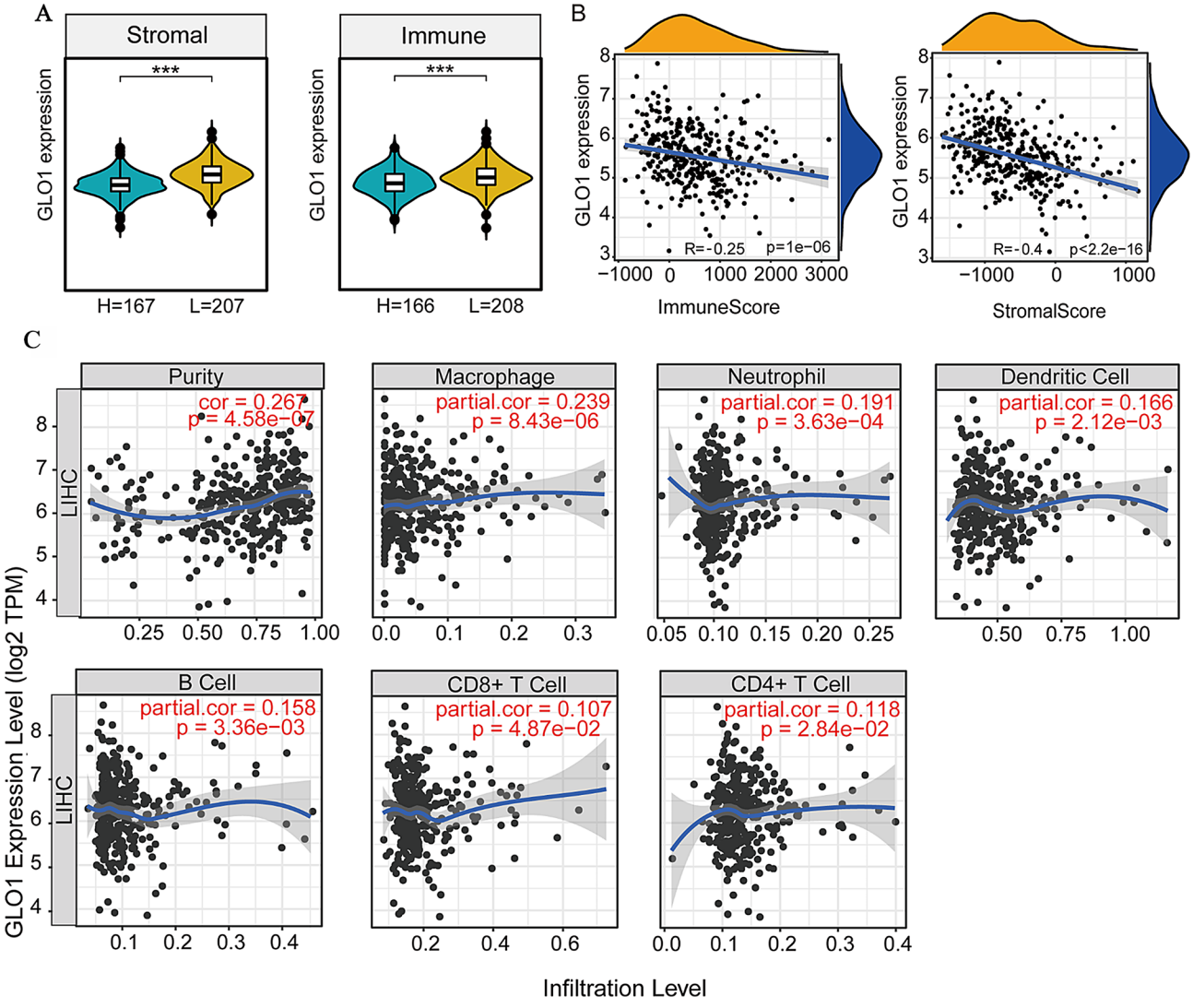

Fig. 2 Analysis of *GLO1* expression and immune cell infiltration in HCC. (**A**) Association of *GLO1* expression levels with differences in immune and stromal scores in HCC. Between the two groups $*p < 0.5$, $**p < 0.01$, $***p < 0.001$. (**B**) Correlation analysis of *GLO1* mRNA expression levels with immune score and stromal score in HCC. (**C**) The relationship between *GLO1* gene expression and the level of infiltration of six types of immune cells in HCC was investigated using the Tumor Immune Estimation Resource (TIMER) database

GLO1 affects the proliferation, migration, and invasion of HCC cells by regulating the cell cycle

To determine how *GLO1* affects cell proliferation and migration, we performed a CCK8 assay. *GLO1* knockout significantly inhibited the proliferation of Hep3B and Huh-7 cells (Fig. 7A), whereas *GLO1* overexpression enhanced proliferation (Fig. 7B). A wound healing assay was performed to analyze the effect of *GLO1* on the migratory ability of HCC cells. We observed attenuated cell migration upon *GLO1* knockout and enhanced cell migration upon *GLO1* overexpression (Fig. 7C-F). According to the transwell invasion assay results, *GLO1*-overexpressing Hep3B and Huh-7 cells had significantly enhanced invasion ability, whereas *GLO1*-knockout cells exhibited significantly reduced invasion ability (Fig. 7G, H). Increased cell proliferation, migration and invasive capacity are key characteristic of cancer development and metastasis. Based on these in vitro findings, we proceeded to validate the role of *GLO1* in HCC cells using an in vivo model.

In vivo validation of the role of *GLO1* in HCC cells

Transparent early zebrafish embryos (AB strain) were used to observe the changes in the growth of fluorescently labeled HCC cells in vivo (Fig. 8A). DiI labeled HCC cells injected into the yolk region of the zebrafish embryos were visualized using fluorescence microscopy (Fig. 8B). The proliferative ability of Hep3B and Huh-7 cells overexpressing *GLO1* was significantly enhanced, whereas that of Hep3B and Huh-7 cells lacking *GLO1*

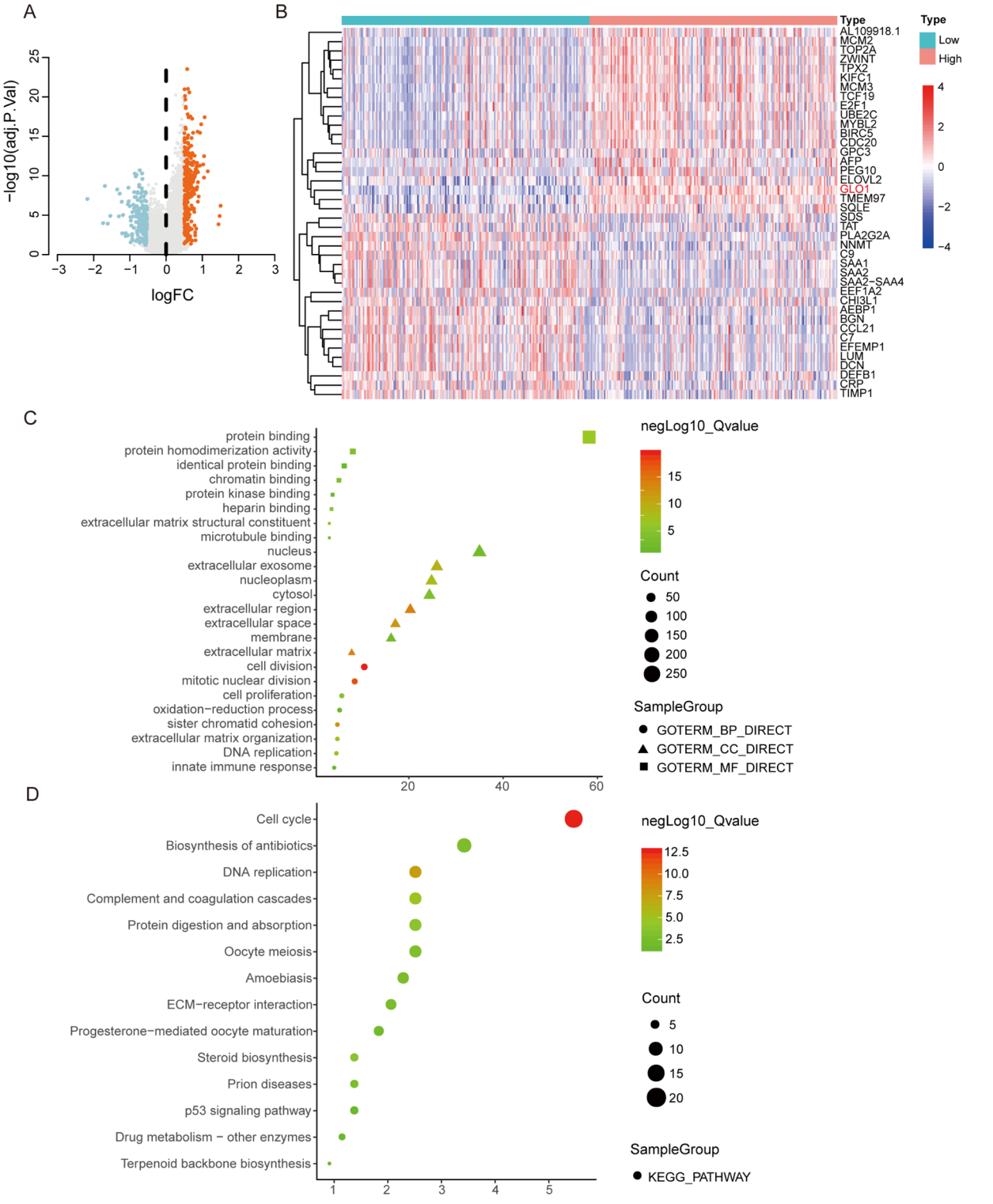

Fig. 3 Identification of DEGs in HCC and GO and KEGG enrichment analysis. (**A**) Volcano plots show the overall distribution of DEGs between the high and low *GLO1* expression groups. (**B**) Heatmap of DEGs generated by comparison between the high and low *GLO1* expression groups. (**C**) GO enrichment analysis of 458 DEGs was conducted via DAVID. GO terms are classified as biological process, cellular component, or molecular function terms. (**D**) KEGG pathway analysis revealed the signaling pathways in which the DEGs were enriched. Each point represents the enrichment level. The color corresponds to -log10 (adjusted p-value), and the size corresponds to the number of enriched genes

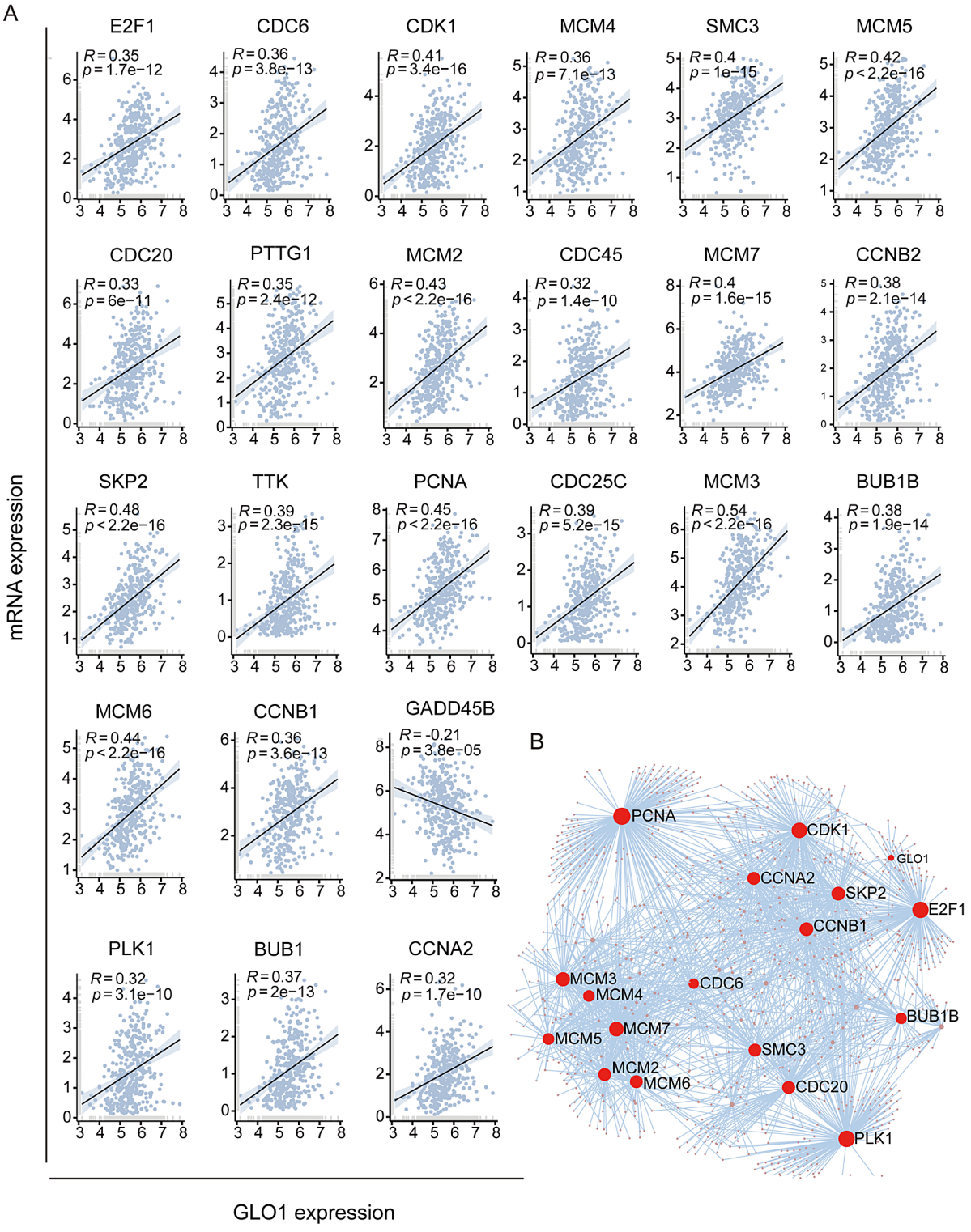

Fig. 4 Correlation analysis and PPI network analysis. (**A**) Correlation analysis of *GLO1* and 24 genes enriched in the cell cycle pathway. (**B**) The PPI network of *GLO1* and 24 cell cycle–related genes was constructed using the NetworkAnalysis tool

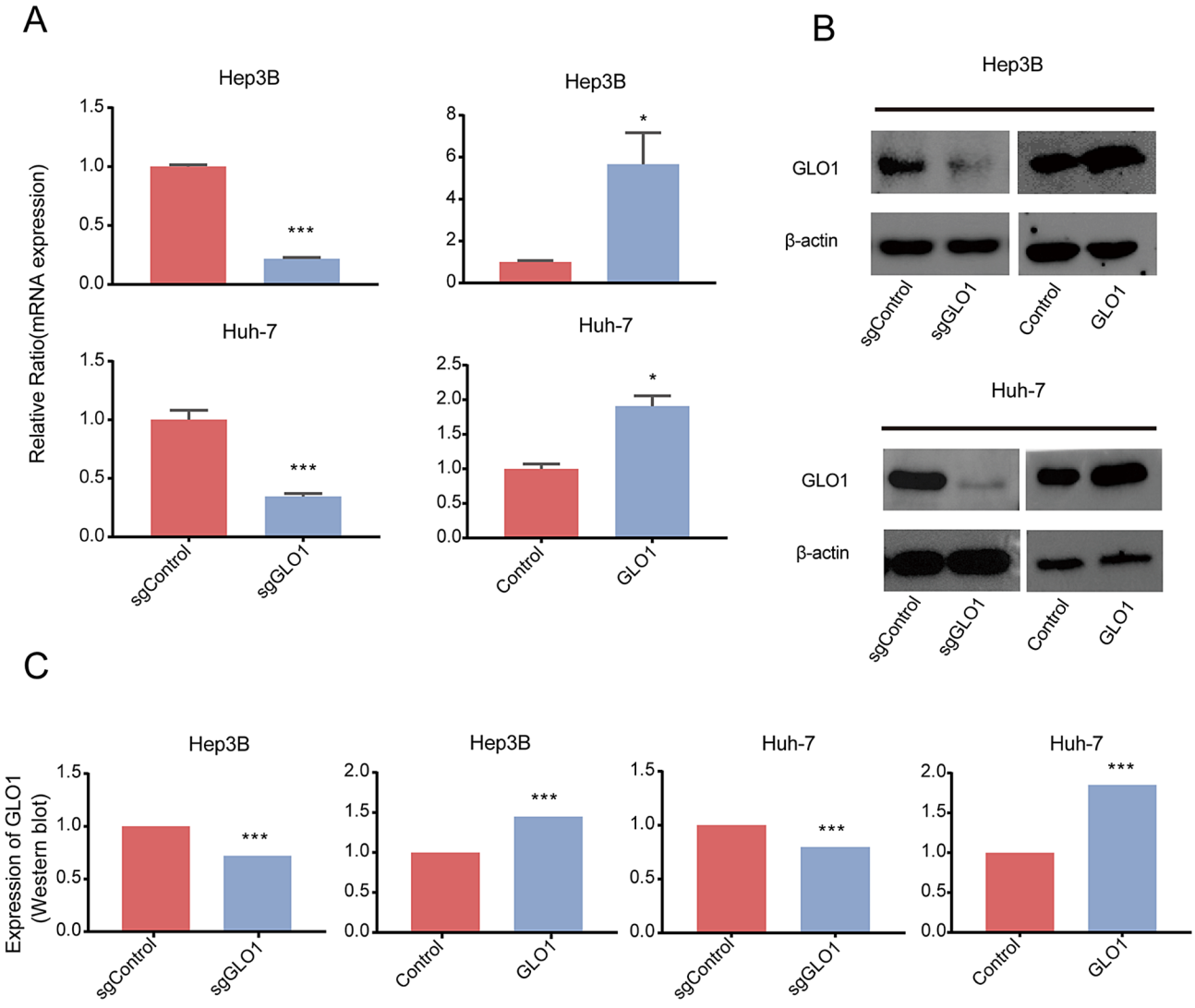

Fig. 5 *GLO1* knockout and overexpression in Hep3B and Huh-7 cells. (**A**) mRNA expression after *GLO1* knockout and overexpression in Hep3B and Huh-7 cell lines was detected by qRT-PCR. (**B**, **C**) Protein expression after *GLO1* knockout and overexpression in Hep3B and Huh-7 cell lines was determined by Western blot analysis (Original version in Supplementary Fig. 3). Statistical significance was determined by t-test: * $p < 0.05$; ** $p < 0.01$; *** $p < 0.001$

was significantly reduced (Fig. 8C). Based on these observations, *GLO1* plays a critical role in promoting the proliferation of HCC cells in vivo, suggesting it as a potential therapeutic target for HCC.

Discussion

In recent years, the incidence of HCC has risen significantly, making it one of the most common cancers. High *GLO1* expression plays a crucial role in tumor initiation and progression [3, 5, 6, 8, 9, 13, 41]. *GLO1* is upregulated in HCC and plays an essential role in HCC cell proliferation, thus presenting itself as a potential therapeutic target [13, 14]. However, comprehensive research on the association between *GLO1* expression and the occurrence and development of HCC remains sparse. This study comprehensively investigated the role of *GLO1* in hepatocellular carcinoma (HCC) and its potential as a therapeutic target. This study investigates the role of GLO1 in HCC and its potential as a therapeutic target through bioinformatics analysis of public data.

Using TCGA data, we evaluated *GLO1* expression in HCC tissues and confirmed that *GLO1* transcription levels were significantly elevated in tumor tissues compared to adjacent normal tissues (Fig. 1A, B, and C), aligning with previous findings [13, 14]. We further examined *GLO1* mutations in HCC at the DNA level, revealing a mutation rate of 4%, though these mutations were not significantly associated with survival (Supplementary Fig. 2). To assess the impact of *GLO1* expression on survival, we analyzed four types of survival data: OS, DFS, DSS, and PFS. *GLO1* expression was significantly associated with the survival rate of HCC patients, suggesting

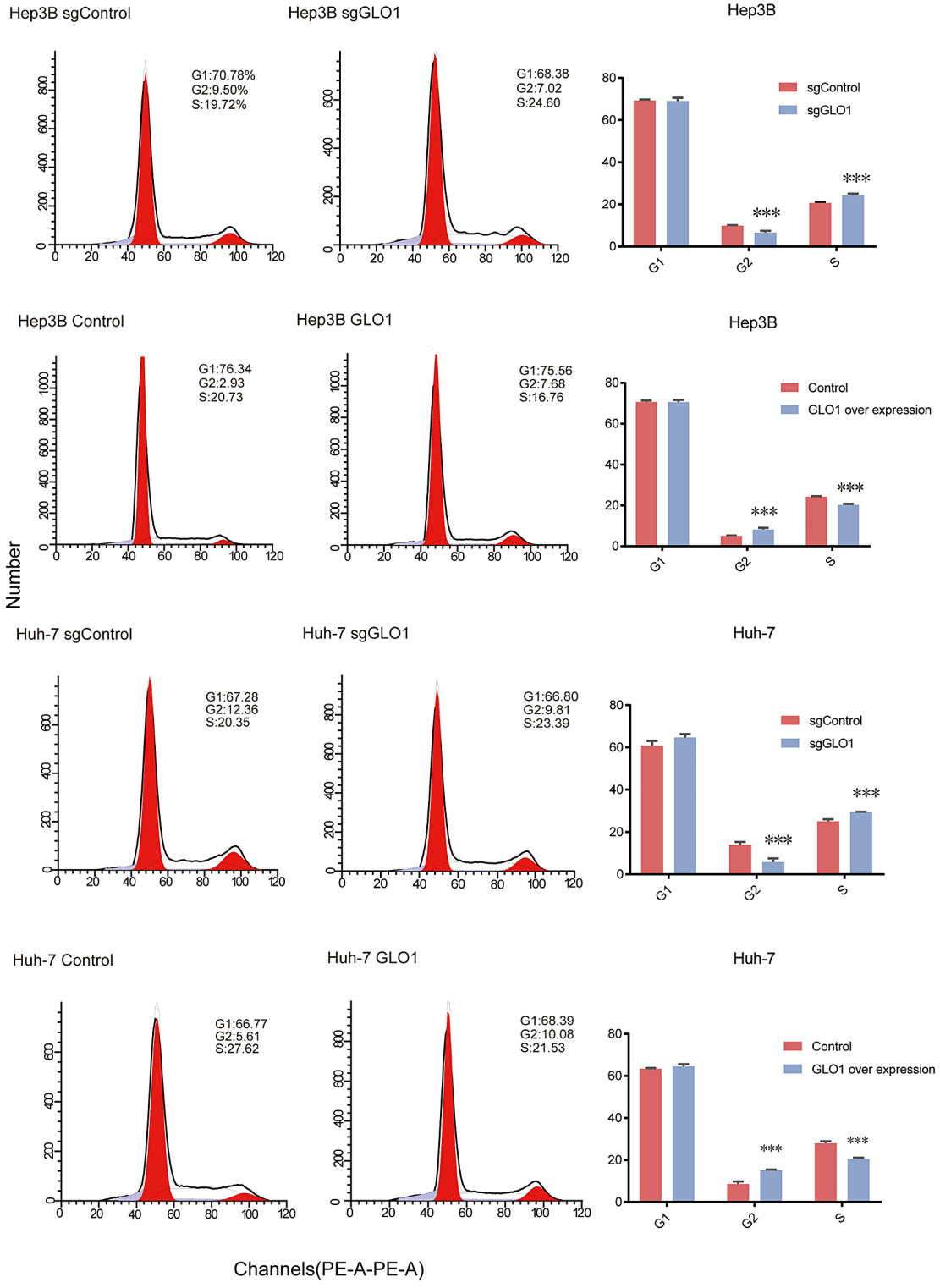

Fig. 6 Effect of *GLO1* knockout and overexpression of HCC cells in each cell cycle stage. *GLO1* knockout and overexpression mainly affected the number of Hep3B and Huh-7 cells in G2 and S phases. Statistical significance was determined by *t*-test: * $p < 0.05$; ** $p < 0.01$; *** $p < 0.001$

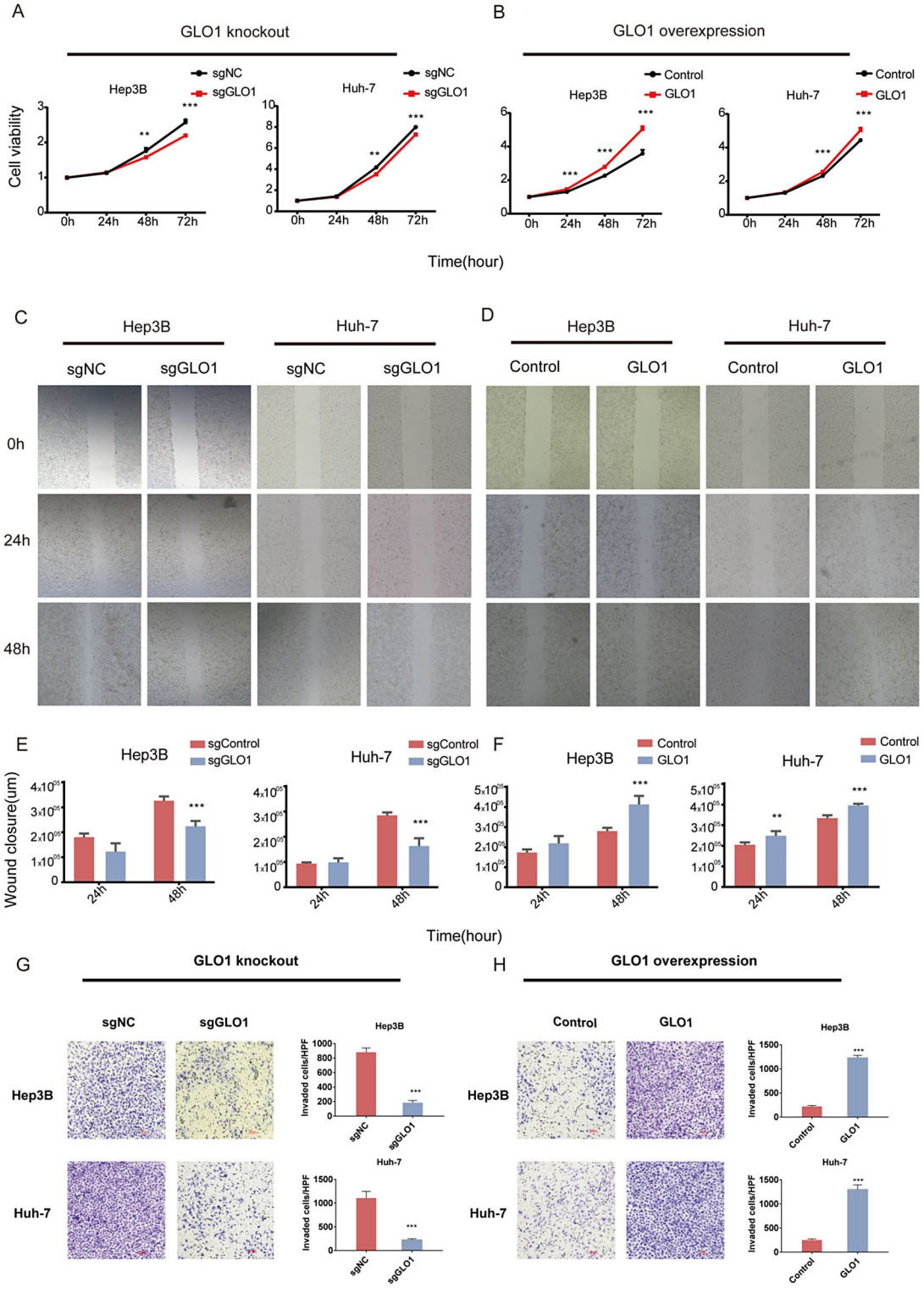

Fig. 7 *GLO1* affects HCC cell proliferation, migration, and invasion by regulating the cell cycle pathway. (**A**, **B**) Proliferative capacity of *GLO1*-knockout and *GLO1*-overexpressing HCC cells was determined by CCK-8 assay. (**C**-**F**) Migration ability of *GLO1*-knockout and *GLO1*-overexpressing HCC cells was determined by wound healing assay. (**G**, **H**) Invasive ability of *GLO1*-knockout and *GLO1*-overexpressing HCC cells was determined by invasion assay. Statistical significance was determined by *t*-test: * $p < 0.05$; ** $p < 0.01$; *** $p < 0.001$

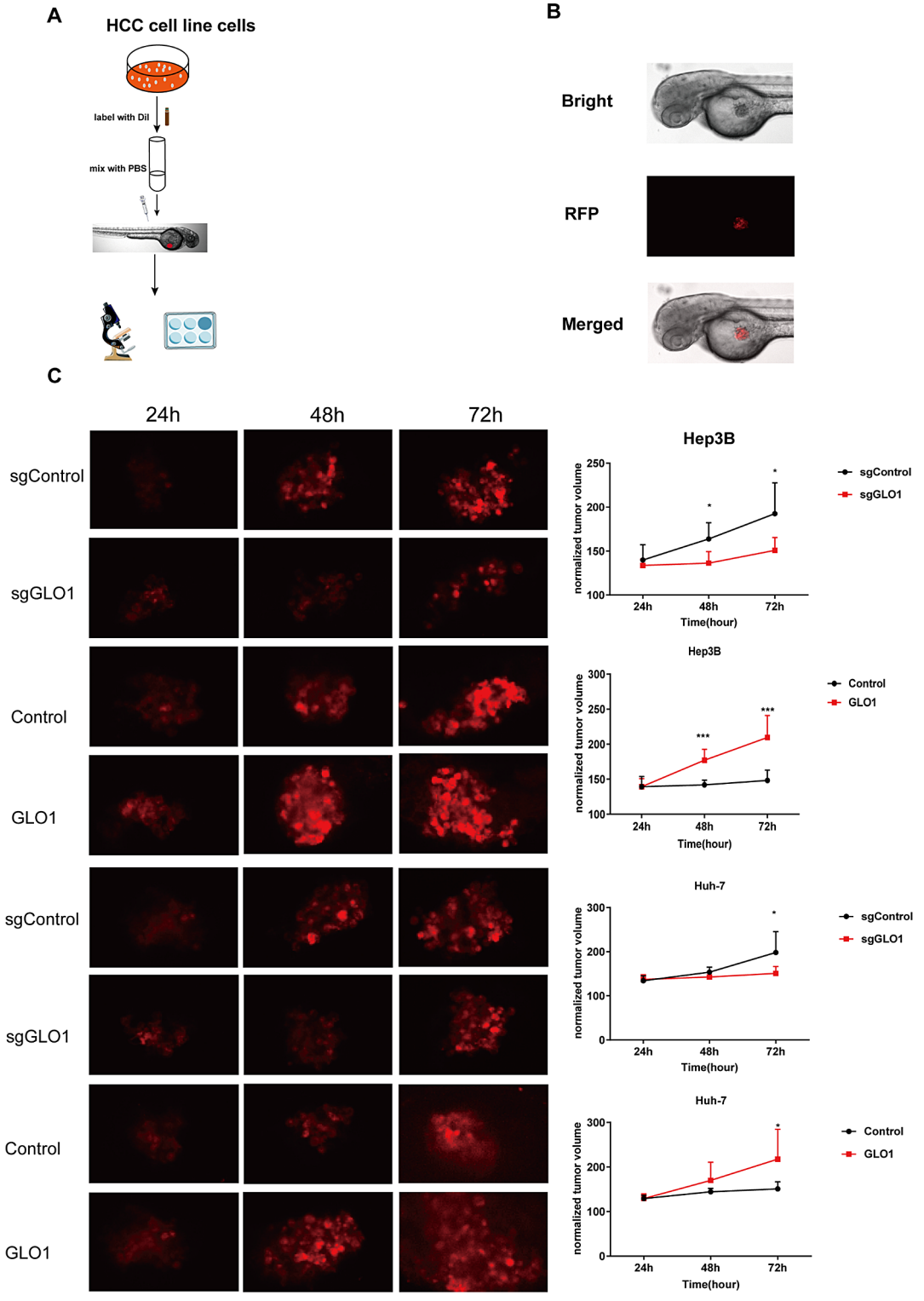

Fig. 8 *GLO1* affects the growth of HCC cells in zebrafish. (**A**) Schematic depicting the procedure for constructing a zebrafish HCC xenograft model. (**B**) Fluorescence microscopy images of DiI stained HCC cells injected into the yolk region of zebrafish. Bright-field microscopy of whole zebrafish (AB line) 24 h after injection of human HCC cells (upper panel). Fluorescence microscopy of DiI stained HCC cells under red fluorescent protein (RFP) channel (middle). Merged bright-field and RFP field microscopy images (bottom). (**C**) Growth of DiI stained HCC cell xenografts in zebrafish

its potential as a prognostic indicator. *GLO1*'s role in promoting tumor proliferation and survival has been highlighted in multiple cancer types, including prostate cancer, breast cancer, pancreatic cancer, malignant melanoma, and gastric cancer [3, 6, 9–12, 41, 42]. *GLO1* expression was not significantly associated with clinicopathological parameters such as grade, age, and sex (Supplementary Fig. 1). *GLO1* is linked to oxidative stress [26], which affects the immune response [30, 37–40]. We speculated that *GLO1* also regulates tumor immunity and found that *GLO1* plays a minor role in HCC immune cell infiltration (Fig. 2).

To investigate the molecular functions of *GLO1* in HCC, we performed GO and KEGG pathway enrichment analysis of DEGs. Enriched BP terms included "cell division" and "mitotic nuclear division" (Fig. 3C). KEGG pathway analysis revealed that the DEGs were mainly enriched in "cell cycle" and "DNA replication" (Fig. 3D). *GLO1* promotes tumor proliferation [3, 10, 14], though the exact mechanism remains unclear. We conducted a correlation analysis between GLO1 expression and genes related to the cell cycle pathway. Specifically, the expression of *E2F1*, *CDC6*, *CDK1*, *SKP2*, *TTK*, *PCNA*, *CDC20*, *PTTG1*, *MCM2*, *CDC25C*, *MCM3*, *BUB1B*, *MCM4*, *SMC3*, *MCM5*, *MCM6*, *CCNB1*, *CDC45*, *MCM7*, *CCNB2*, *PLK1*, *BUBI*, and *CCNA2* was positively correlated with *GLO1* expression, whereas *GADD45B* expression was negatively correlated (Fig. 4A). Given that alterations in cell cycle regulation are known to drive tumor proliferation and survival by enabling cancer cells to bypass normal growth constraints and evade apoptosis [43]. We hypothesize that GLO1 may contribute to tumor proliferation and viability by activating the cell cycle pathway. *GLO1* expression was significantly correlated with that of genes enriched in the cell cycle pathway (Fig. 4A). However, this does not establish a causal relationship between *GLO1* and cell cycle pathway activation. Therefore, we constructed a *GLO1* knockout and overexpression system for further validation. *GLO1* expression predominantly influenced the number of cells in G2 and S phase of the cell cycle (Fig. 6), supporting previous reports that *GLO1*'s role in tumor proliferation and survival [5, 7, 8, 14]. The results demonstrated that *GLO1* affects the proliferation and migration of HCC cells by regulating the cell cycle (Fig. 7).

In conclusion, this study provides comprehensive evidence supporting *GLO1*'s pivotal role in HCC development. Our findings indicate that *GLO1* is overexpressed in HCC tissues and is associated with a poor prognosis, similar to other human malignancies [44]. Furthermore, our findings elucidate that overexpression of *GLO1* activates the cell cycle pathway and correlates with genes enriched in this pathway. Experimental validation indicated that *GLO1* expression affects the number of HCC cells in G2 and S phases and regulates HCC cell proliferation and migration. These results underscore *GLO1* as a promising therapeutic target for HCC, offering valuable insights into its role in tumor viability and proliferation. Future directions include further elucidation of the underlying molecular mechanisms and validation of *GLO1*-targeted therapeutic strategies in clinical settings.

Abbreviations

DFS	Disease-free survival
DSS	Disease-specific survival
GEO	Gene Expression Omnibus
GO	Gene Ontology
GLO1	Glyoxalase-1
HBV	Hepatitis B virus
HCC	Hepatocellular carcinoma
HCV	Hepatitis C virus
KEGG	Kyoto Encyclopedia of Genes and Genomes
OS	Overall survival
PFS	Progression-free survival
PPI	Protein-protein interaction
TCGA	The Cancer Genome Atlas

Supplementary Information

The online version contains supplementary material available at https://doi.org/10.1186/s12885-024-12927-x.

Supplementary Material 1

Supplementary Material 2

Supplementary Material 3

Supplementary Material 4

Acknowledgements

Not applicable.

Author contributions

F.K.D, Z.G.X, and L.Y, Designed the experiments. Y.Z, X.L.T, L.L, D.C, S.G, S.Y.H, and Y.L, Analyzed the data and performed the experiments. J.S, Y.C, Y.S.Z, X.W, M.X.L, M.J.C, X.B.L, Y.H.S, L.G, W.P.L, F.W, Z.Z, X.D.W, and S.D, Supervised the study and coordinated the writing of the manuscript.

Funding

This study was supported by grants from the Sichuan Science and Technology Program, China (No. 2022NSFSC0783, No. 2022YFS0619), the Joint Founds of Southwest Medical University and Luzhou Government (No.2020LZXNYDJ08), Grants of Southwest Medical University (2021ZKMS038), Funds of talent introduction and scientific research of Southwest Medical University (No.05-00040140), The Project of Science and Technology Department of Sichuan Provincial of China to L.Y. (2019JDJQ0035).

Data availability

GLO1 expression levels and clinical HCC data were obtained from The Cancer Genome Atlas (TCGA) (http://cancergenome.nih.gov) [31]. Standardized TCGA and GTEX transcriptome data from normal tissue ($N=160$) and tumor tissue ($N=374$) samples were retrieved from the UCSC database (https://xenabrowser.net/). The datasets GSE45436 ($N=39$, $T=95$), GSE57957 ($N=39$, $T=39$), and GSE76427 ($N=52$, $T=115$), containing liver cancer sequencing data, were downloaded from the Gene Expression Omnibus (GEO) database (http://www.ncbi.nlm.nih.gov/geo/).

Declarations

Ethics approval and consent to participate
The study was performed in accordance with the relevant guidelines and regulations. All animal protocols were approved by the Ethics Committee of Southwest Medical University (Date: February 24, 2021/No.: 20210223-243). This research was in accordance with ARRIVE guidelines.

Consent for publication
Not applicable.

Competing interests
The authors declare no competing interests.

Author details
[1]Laboratory of Molecular Pharmacology, Department of Pharmacology, School of Pharmacy, Southwest Medical University, Luzhou, Sichuan 646000, China
[2]Cell Therapy & Cell Drugs of Luzhou Key Laboratory, Luzhou, Sichuan 646000, China
[3]South Sichuan Institute of Translational Medicine, Luzhou, Sichuan 646000, China
[4]Department of Oncology, Affiliated Hospital of Southwest Medical University, Luzhou, Sichuan 646000, China
[5]Public Center of Experimental Technology, Southwest Medical University, Luzhou, Sichuan 646000, China
[6]Key Laboratory of Luzhou City for Aging Medicine, School of Pharmacy, Southwest Medical University, Luzhou, Sichuan 646000, China
[7]Department of Hepatobiliary Disease, The Affiliated Traditional Chinese Medicine Hospital, Southwest Medical University, Luzhou, Sichuan 646000, China
[8]The Key Laboratory for Human Disease Gene Study of Sichuan Province and Department of Laboratory Medicine, Sichuan Provincial People's Hospital, School of Medicine, University of Electronic Science and Technology of China, Chengdu 610072, China
[9]Research Unit for Blindness Prevention of Chinese Academy of Medical Sciences (2019RU026), Sichuan Academy of Medical Sciences, Chengdu 610072, China

Received: 6 July 2023 / Accepted: 10 September 2024
Published online: 21 October 2024

References

1. Jandova J, Wondrak GT. Genomic GLO1 deletion modulates TXNIP expression, glucose metabolism, and redox homeostasis while accelerating human A375 malignant melanoma tumor growth. Redox Biol. 2021;39:101838.
2. Chiavarina B, Nokin MJ, Bellier J, Durieux F, Bletard N, Sherer F, Lovinfosse P, Peulen O, Verset L, Dehon R et al. Methylglyoxal-mediated stress correlates with high metabolic activity and promotes Tumor Growth in Colorectal Cancer. Int J Mol Sci 2017;18(1).
3. Hutschenreuther A, Bigl M, Hemdan NY, Debebe T, Gaunitz F, Birkenmeier G. Modulation of GLO1 expression affects malignant properties of cells. Int J Mol Sci 2016;17(12).
4. Luengo A, Abbott KL, Davidson SM, Hosios AM, Faubert B, Chan SH, Freinkman E, Zacharias LG, Mathews TP, Clish CB, et al. Reactive metabolite production is a targetable liability of glycolytic metabolism in lung cancer. Nat Commun. 2019;10(1):5604.
5. Tian X, Wang Y, Ding X, Cheng W. High expression of GLO1 indicates unfavorable clinical outcomes in glioma patients. J Neurosurg Sci 2019.
6. Burdelski C, Shihada R, Hinsch A, Angerer A, Gobel C, Friedrich E, Hube-Magg C, Burdak-Rothkamm S, Kluth M, Simon R, et al. High-level glyoxalase 1 (GLO1) expression is linked to poor prognosis in prostate cancer. Prostate. 2017;77(15):1528–38.
7. Santarius T, Bignell GR, Greenman CD, Widaa S, Chen L, Mahoney CL, Butler A, Edkins S, Waris S, Thornalley PJ, et al. GLO1-A novel amplified gene in human cancer. Genes Chromosomes Cancer. 2010;49(8):711–25.
8. Bair WB 3rd, Cabello CM, Uchida K, Bause AS, Wondrak GT. GLO1 overexpression in human malignant melanoma. Melanoma Res. 2010;20(2):85–96.
9. Wang Y, Kuramitsu Y, Ueno T, Suzuki N, Yoshino S, Iizuka N, Akada J, Kitagawa T, Oka M, Nakamura K. Glyoxalase I (GLO1) is up-regulated in pancreatic cancerous tissues compared with related non-cancerous tissues. Anticancer Res. 2012;32(8):3219–22.
10. Cheng WL, Tsai MM, Tsai CY, Huang YH, Chen CY, Chi HC, Tseng YH, Chao IW, Lin WC, Wu SM, et al. Glyoxalase-I is a novel prognosis factor associated with gastric cancer progression. PLoS ONE. 2012;7(3):e34352.
11. Antognelli C, Marinucci L, Frosini R, Macchioni L, Talesa VN. Metastatic prostate Cancer cells secrete methylglyoxal-derived MG-H1 to reprogram human osteoblasts into a dedifferentiated, malignant-like phenotype: a possible novel player in prostate Cancer bone metastases. Int J Mol Sci 2021, 22(19).
12. Antognelli C, Mandarano M, Prosperi E, Sidoni A, Talesa VN. Glyoxalase-1-Dependent methylglyoxal depletion sustains PD-L1 expression in metastatic prostate Cancer cells: a novel mechanism in Cancer Immunosurveillance escape and a potential Novel Target to Overcome PD-L1 Blockade Resistance. Cancers 2021, 13(12).
13. Zhang S, Liang X, Zheng X, Huang H, Chen X, Wu K, Wang B, Ma S. Glo1 genetic amplification as a potential therapeutic target in hepatocellular carcinoma. Int J Clin Exp Pathol. 2014;7(5):2079–90.
14. Hu X, Yang X, He Q, Chen Q, Yu L. Glyoxalase 1 is up-regulated in hepatocellular carcinoma and is essential for HCC cell proliferation. Biotechnol Lett. 2014;36(2):257–63.
15. Sung H, Ferlay J, Siegel RL, Laversanne M, Soerjomataram I, Jemal A, Bray F. Global Cancer statistics 2020: GLOBOCAN estimates of incidence and Mortality Worldwide for 36 cancers in 185 countries. CA Cancer J Clin. 2021;71(3):209–49.
16. Donato F, Gelatti U, Tagger A, Favret M, Ribero ML, Callea F, Martelli C, Savio A, Trevisi P, Nardi G. Intrahepatic cholangiocarcinoma and hepatitis C and B virus infection, alcohol intake, and hepatolithiasis: a case-control study in Italy. Cancer Causes Control: CCC. 2001;12(10):959–64.
17. Marengo A, Rosso C, Bugianesi E. Liver Cancer: connections with obesity, fatty liver, and cirrhosis. Annu Rev Med. 2016;67:103–17.
18. Grandhi MS, Kim AK, Ronnekleiv-Kelly SM, Kamel IR, Ghasebeh MA, Pawlik TM. Hepatocellular carcinoma: from diagnosis to treatment. Surg Oncol. 2016;25(2):74–85.
19. Li L, Wang H. Heterogeneity of liver cancer and personalized therapy. Cancer Lett. 2016;379(2):191–7.
20. Wang Z, Li Z, Ye Y, Xie L, Li W. Oxidative Stress and Liver Cancer: Etiology and Therapeutic Targets. Oxid Med Cell Longev. 2016;2016:7891574.
21. Shen J, Chen M, Lee D, Law CT, Wei L, Tsang FH, Chin DW, Cheng CL, Lee JM, Ng IO, et al. Histone chaperone FACT complex mediates oxidative stress response to promote liver cancer progression. Gut. 2020;69(2):329–42.
22. Liu MX, Jin L, Sun SJ, Liu P, Feng X, Cheng ZL, Liu WR, Guan KL, Shi YH, Yuan HX, et al. Metabolic reprogramming by PCK1 promotes TCA cataplerosis, oxidative stress and apoptosis in liver cancer cells and suppresses hepatocellular carcinoma. Oncogene. 2018;37(12):1637–53.
23. McLoughlin MR, Orlicky DJ, Prigge JR, Krishna P, Talago EA, Cavigli IR, Eriksson S, Miller CG, Kundert JA, Sayin VI, et al. TrxR1, gsr, and oxidative stress determine hepatocellular carcinoma malignancy. Proc Natl Acad Sci USA. 2019;116(23):11408–17.
24. Lee D, Xu IM, Chiu DK, Leibold J, Tse AP, Bao MH, Yuen VW, Chan CY, Lai RK, Chin DW, et al. Induction of oxidative stress through inhibition of Thioredoxin Reductase 1 is an effective Therapeutic Approach for Hepatocellular Carcinoma. Hepatology. 2019;69(4):1768–86.
25. Marra M, Sordelli IM, Lombardi A, Lamberti M, Tarantino L, Giudice A, Stiuso P, Abbruzzese A, Sperlongano R, Accardo M, et al. Molecular targets and oxidative stress biomarkers in hepatocellular carcinoma: an overview. J Translational Med. 2011;9:171.
26. Wang Z, Zhang J, Chen L, Li J, Zhang H, Guo X. Glycine Suppresses AGE/RAGE Signaling Pathway and Subsequent Oxidative Stress by Restoring Glo1 Function in the Aorta of Diabetic Rats and in HUVECs. Oxid Med Cell Longev. 2019;2019:4628962.
27. Antognelli C, Trapani E, Delle Monache S, Perrelli A, Fornelli C, Retta F, Cassoni P, Talesa VN, Retta SF. Data in support of sustained upregulation of adaptive redox homeostasis mechanisms caused by KRIT1 loss-of-function. Data Brief. 2018;16:929–38.
28. Delle Monache S, Pulcini F, Frosini R, Mattei V, Talesa VN, Antognelli C. Methylglyoxal-dependent glycative stress is prevented by the natural antioxidant oleuropein in Human Dental Pulp Stem Cells through Nrf2/Glo1 pathway. Antioxidants 2021, 10(5).
29. Gambelunghe A, Giovagnoli S, Di Michele A, Boncompagni S, Dell'Omo M, Leopold K, Iavicoli I, Talesa VN, Antognelli C. Redox-Sensitive glyoxalase 1 Up-Regulation is crucial for protecting human lung cells from gold nanoparticles toxicity. Antioxidants 2020;9(8).

30. Du F, Li Y, Shen J, Zhao Y, Kaboli PJ, Xiang S, Wu X, Li M, Zhou J, Zheng Y, et al. Glyoxalase 1 gene improves the antistress capacity and reduces the immune inflammatory response. BMC Genet. 2019;20(1):95.
31. Tomczak K, Czerwinska P, Wiznerowicz M. The Cancer Genome Atlas (TCGA): an immeasurable source of knowledge. Contemp Oncol. 2015;19(1A):A68–77.
32. Wu P, Heins ZJ, Muller JT, Katsnelson L, de Bruijn I, Abeshouse AA, Schultz N, Fenyo D, Gao J. Integration and analysis of CPTAC Proteomics Data in the context of Cancer Genomics in the cBioPortal. Mol Cell Proteomics: MCP. 2019;18(9):1893–8.
33. Therneau T, Grambsch P. Modeling Survival Data: extending the Cox Model. New York, NY: Springer; 2000.
34. Yoshihara K, Shahmoradgoli M, Martinez E, Vegesna R, Kim H, Torres-Garcia W, Trevino V, Shen H, Laird PW, Levine DA, et al. Inferring tumour purity and stromal and immune cell admixture from expression data. Nat Commun. 2013;4:2612.
35. Li T, Fan J, Wang B, Traugh N, Chen Q, Liu JS, Li B, Liu XS. TIMER: a web server for Comprehensive Analysis of Tumor-infiltrating Immune cells. Cancer Res. 2017;77(21):e108–10.
36. Zhou G, Soufan O, Ewald J, Hancock REW, Basu N, Xia J. NetworkAnalyst 3.0: a visual analytics platform for comprehensive gene expression profiling and meta-analysis. Nucleic Acids Res. 2019;47(W1):W234–41.
37. Datta S, Cano M, Ebrahimi K, Wang L, Handa JT. The impact of oxidative stress and inflammation on RPE degeneration in non-neovascular AMD. Prog Retin Eye Res. 2017;60:201–18.
38. Dietz RM, Wright CJ. Oxidative stress diseases unique to the perinatal period: a window into the developing innate immune response. Am J Reprod Immunol. 2018;79(5):e12787.
39. Laddha NC, Dwivedi M, Mansuri MS, Gani AR, Ansarullah M, Ramachandran AV, Dalai S, Begum R. Vitiligo: interplay between oxidative stress and immune system. Exp Dermatol. 2013;22(4):245–50.
40. Zhang B, Zehnder JL. Oxidative stress and immune thrombocytopenia. Semin Hematol. 2013;50(3):e1–4.
41. Lv N, Hao S, Luo C, Abukiwan A, Hao Y, Gai F, Huang W, Huang L, Xiao X, Eichmuller SB, et al. miR-137 inhibits melanoma cell proliferation through downregulation of GLO1. Sci China Life Sci. 2018;61(5):541–9.
42. Antognelli C, Cecchetti R, Riuzzi F, Peirce MJ, Talesa VN. Glyoxalase 1 sustains the metastatic phenotype of prostate cancer cells via EMT control. J Cell Mol Med. 2018;22(5):2865–83.
43. Evan GI, Vousden KH. Proliferation, cell cycle and apoptosis in cancer. Nature. 2001;411(6835):342–8.
44. Antognelli C, Talesa VN. Glyoxalases in Urological malignancies. Int J Mol Sci 2018, 19(2).

Publisher's note